

# Dissipation rates from experimental uncertainty

Aishani Ghosal<sup>1,2</sup> and Jason R. Green<sup>1,2,\*</sup>

<sup>1</sup>*Department of Chemistry, University of Massachusetts Boston, Boston, MA 02125 USA*

<sup>2</sup>*Department of Physics, University of Massachusetts Boston, Boston, MA 02125 USA*

(Dated: December 19, 2024)

Active matter and driven systems exhibit statistical fluctuations in density and particle positions, providing an indirect indicator of dissipation across multiple length and time scales. Here, we quantitatively relate these measurable fluctuations to a thermodynamic speed limit that constrains the rates of heat and entropy production in nonequilibrium processes. By reparametrizing the speed limit, we show how to infer heat and entropy production rates from directly observable or controllable quantities. This approach can use available experimental data and avoid the need for analytically solvable microscopic models or full time-dependent probability distributions. The heat rate we predict agrees with experimental measurements for a Brownian particle and a microtubule active gel, which validates the approach and suggests potential for the design of experiments.

*Introduction.*— Dissipation rates determine the efficiency of biological processes [1, 2] and are now an important feature in designing active synthetic materials that function [3–10]. For example, active cytoskeletal materials sustain self-organized flows by consuming chemical energy and dissipating heat at picowatt rates [11]. It recently became possible to measure these rates with advances in picocalorimetry [12] and to directly observe active materials in the liquid phase with high-resolution electron microscopy [13]. These techniques are able to resolve dissipative degrees of freedom and beginning to provide a better understanding of how chemical energy propagates up length and timescales. However, these measurements are often interpreted with empirical models of the kinetics, which can have large uncertainties, missing parameters, and modeling assumptions that may be unjustified for active materials (e.g., well-mixed chemical kinetics, modeling only rate limiting reactions) [14]. Model-free approaches to predict dissipation rates from available experimental data could guide this experimentation on functional materials and their design [15–17].

Surveying stochastic thermodynamics [18], the thermodynamic speed limit [19] set by the Fisher information [20–22]  $I_F = \tau^{-2}$  has potential for estimating dissipation rates. While not yet experimentally tested, this single timescale upper bounds the rate of heat, entropy production, dissipated work, chemical work [19, 23–25]. For example, a system that dissipates energy as heat with a rate  $\dot{Q}$  [26] and is subject to energy fluctuations with a standard deviation  $\Delta\epsilon$  has the speed limit [19],

$$\tau_Q^{-1} := \frac{|\dot{Q}|}{\Delta\epsilon} \leq \sqrt{I_F} =: \tau^{-1}, \quad (1)$$

even if work is done on or by the system [27]. Speed limits on dissipation rates are now known in quantum [28–30], classical deterministic [31, 32], and stochastic [19, 33–35] dynamics. Alternative approaches to infer dissipation, such as the dissipation-time uncertainty relation [36] or the thermodynamic uncertainty relation [37–44] and its extensions [45, 46] estimate dissipa-

tion through the statistics of currents [47]. Others use optimization methods and transition rates [48, 49], waiting times [48, 50], variances [51, 52], partial information, and coarse-graining [53, 54]. However, these approaches give lower bounds on entropy production rates that are not necessarily explicit functions of easily measurable observables or estimates of the energy dissipated as heat. By contrast, estimates of the Fisher information in Eq. (1) could give upper bounds on the maximum rate of dissipation of entropy and heat. Eq. (1) is also unique in that it can be combined with the quantum time-energy uncertainty relation [55] to bound the dynamical observables of open quantum systems [56].

In this Letter, we establish a method for predicting the rates of nonequilibrium observables from experimental data through the thermodynamic speed limit in Eq. (1). The Fisher information enables us to use measurements of uncertainty as input. Both classical and quantum Fisher information are part of the statistical design of experiments on systems ranging from chemical reactions and biological populations to dark matter [57]; by measuring experimental errors, one can use the Fisher information (matrix) to predict *a priori* the minimum error of any measured quantity [58]. In this context, the Fisher information predicts the minimum error in an observable before the measurement, which can then be used to assess the measurement sensitivity to control variables, minimize errors, and improve the precision. Here, we establish a similar framework for inferring dissipation rates, transforming the coordinates of the Fisher information so that we can use available measurements of positions, concentrations, and control variables [11]. Our predictions confirm experimentally measured dissipation rates in several examples, including an active cytoskeleton materials composed of kinesin motors and microtubules [11] measured with picocalorimetry [12].

*Predicting dissipated heat by transforming the speed limit.*— To illustrate the approach, first consider the net rate of heat generation  $|\dot{Q}|$  when dragging an optically trapped colloidal particle at a speed  $|v|$  through a vis-

cous medium at a temperature  $T$ , Fig. 1. The position fluctuates with a standard deviation  $\sigma_x$  that converges to a finite value at nonequilibrium steady state. We consider the case in which the true position distribution is unknown but one can estimate statistical parameters by repeated measurements. In this case, repeatedly measuring the spatial location of the particle using an estimator  $\hat{x}$  will lead to an empirical standard deviation  $\Delta\hat{x} = \sigma_x \pm |\varepsilon|$  with measurement error  $\varepsilon$ . We denote estimators of directly measured variables  $\hat{\theta}$  to distinguish them from the true values  $\theta$  and those predicted  $\hat{\theta}$ .

At first glance, determining the speed limit set by the Fisher information seems to require the probability distribution  $\rho(x, t)$  from experiments or a microscopic model for the dynamics of the particle. The measured positions  $x_i$  depend on the unknown distribution  $\rho(x, t)$  moving through space at an unknown intrinsic rate  $\hat{r} = -\partial_t \ln \rho(x, t)$  – a nonzero quantity in the lab frame at nonequilibrium steady state. However, because the Fisher information is a variance  $\Delta\hat{r}^2$ , we can change its coordinates and effectively propagate the error from the uncertainty in the particle position (Supplementary Material, SM Sec. 1). Through this coordinate transformation, a direct measurement of  $\Delta\hat{x}$  can serve as an indirect measurement  $\tilde{\tau}^{-1} = \Delta\hat{r}$  of the true speed limit in Eq. (1).

To relate the speed limit to data, we recognize that the fluctuations in position  $\Delta\hat{x}$  propagate [59] to  $\Delta\hat{r}$ . Since the estimator  $\hat{r}$  is a function  $\hat{r} = f(\hat{x})$ , the speed limit is

$$\tilde{\tau}^{-1} := \Delta\hat{r} = \frac{\Delta\hat{x}}{|\partial_f \hat{x}|} + \mathcal{O}(\Delta\hat{x}^2). \quad (2)$$

Rearranging to  $\Delta\hat{x}^2 = (\partial_f \hat{x})\tilde{\tau}^{-2}(\partial_f \hat{x})$ , we can also recognize that the uncertainty in position is a coordinate transformation of the Fisher information. This transformation is a special case of our main result: it relates measurable uncertainties to the speed limit, which can enable estimates of the speed limit without a dynamical model for the probability distribution.

When the dynamics are unknown, we can find the derivatives in Eq. (2) using regression techniques. By hypothesizing the relationship between the rate  $\hat{r} = f(\hat{x})$  [23] and chosen observable  $\hat{x}$ , we can minimize the mean squared error to find the optimal parameters and the derivatives [60]. For example, hypothesizing a linear relationship  $f(\hat{x}) = a + b\hat{x}$ , the optimal slope is  $b_{\text{opt}} = \partial_{\hat{x}} f = v/\Delta\hat{x}^2$  (SM Sec. 2). Using the result in Eq. (2), the speed limit  $\tilde{\tau}^{-1} = |v|/\Delta\hat{x}$  is in terms of the pulling speed and sample variance  $\Delta\hat{x}$ .

With direct measurements or estimates of the position fluctuations, we can also use the speed limit to predict the heat rate (SM Sec. 3) and other nonequilibrium observables. Notice that we can isolate the heat rate in Eq. (1):  $|\dot{Q}| = \tau_Q^{-1}\Delta\epsilon$ . If we similarly find the measured heat rate  $\tilde{Q}$  using Eq. (2) and estimating  $\tilde{\tau}_Q^{-1}\Delta\epsilon \approx \tilde{\tau}^{-1}\Delta\epsilon$ . For the pulled particle, the heat rate at nonequilibrium steady

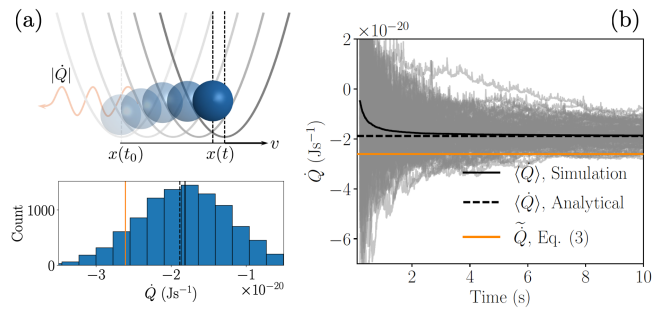


Figure 1. (a) A Brownian particle dissipates energy as heat when pulled through a viscous medium. At  $t = t_0$ , the particle is at the trap center  $x(t_0)$ . Translating the trap through space forces the average particle position to be higher on the potential. During the process, heat is dissipated at a rate  $|\dot{Q}|$  into the environment. (b) Histogram of the heat dissipated to the environment from a simulation of the overdamped Langevin dynamics for 10,000 noise realizations at  $t = 4$  s (SM Sec. 2). The housekeeping heat rate from Eq. (3) (orange) agrees with the sample mean from the simulations (black solid line) and the analytical mean (black dotted line).

state

$$|\tilde{Q}| = \tilde{\tau}_Q^{-1}\Delta\epsilon \approx |v|\Delta\epsilon/\Delta\hat{x}, \quad (3)$$

is in terms of known quantities from the experimental setup: the pulling speed and the uncertainties in the particle position and energy. In the lab frame, this heat rate is the housekeeping contribution that maintains the nonequilibrium steady state [26].

From Eq. (3), we can predict the heat rate using available experimental parameters. Take a particle of radius  $1 \mu\text{m}$  being pulled at a speed [61]  $|v| = 1 \mu\text{m s}^{-1}$  through water. If the standard deviations in Eq. (3) are obtained from measurements, they can be directly used to calculate the heat rate without additional assumptions. However, provided the surrounding medium is at thermal equilibrium, the standard deviation in position is known [62] to be  $\Delta\hat{x} \approx \sigma_x = \sqrt{k_B T/k_f} = 78.32 \text{ nm}$  (errors can be of order  $\pm 2 \text{ nm}$  [61]), and the standard deviation in energy is  $\Delta\epsilon \approx k_B T/2$ . We take the trap to be harmonic with a force constant  $k_f = 6.67 \times 10^{-7} \text{ N m}^{-1}$  and the surrounding medium to be water with a viscosity  $\eta = 10^{-3} \text{ Pa s}$  at  $296.5 \text{ K}$  [63]. Using only these experimental values, the heat rate from Eq. (3) is  $|\tilde{Q}| = |v|\sqrt{k_f/\beta} = 2.61 \times 10^{-20} \text{ W}$ .

To confirm this value, we chose physical models for the dynamics of the particle at the same experimental conditions. We numerically simulated a particle undergoing Brownian dynamics and, over time, measured the particle position relative to the trap center in the laboratory frame [64] [65]. As shown in Fig. 1, the housekeeping heat rate from Eq. (3) agrees well with the average over noise realizations from our numerical simulations  $1.85 \times 10^{-20} \text{ W}$ . It also agrees well with an ana-

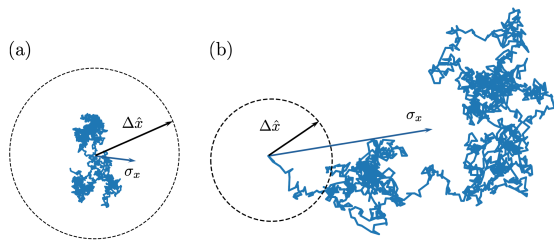


Figure 2. Illustration showing the spatial resolution of experimental measurements compared to the intrinsic fluctuations of a particle undergoing Brownian motion. (a) A lower resolution (higher uncertainty,  $\Delta\hat{x}$ ) than required to measure position fluctuations  $\sigma_x$  of a Brownian particle leads to an upper bound on the speed limit,  $\tilde{\tau}^{-1} \leq \tau^{-1}$ . (b) A higher resolution (lower uncertainty) than required to measure position fluctuations leads to a lower bound,  $\tilde{\tau}^{-1} \geq \tau^{-1}$ .

lytical prediction [61] for the heat rate  $|\langle\dot{Q}\rangle| = v^2/\gamma = 1.885 \times 10^{-20}$  W (SM Sec 2).

*Thermodynamic speed limits from experimental uncertainty.*—As this example highlights, the coordinate transformation of the Fisher information, together with a regression hypothesis for the relationship between  $\hat{r}$  and  $\hat{x}$ , can bypass the need for the full probability distribution of a dynamical model. This observation motivated us to derive a more general framework for measuring this speed limit by transforming the Fisher information into the variance of other measurable quantities.

Take  $\mathbf{X}$  to be a vector of quantities that are measurable by experiment. Because of their statistical fluctuations, we can model these quantities as random variables with means  $\boldsymbol{\mu}$  and covariances  $(\mathbf{C}_X)_{ij} = \text{cov}(X_i, X_j)$ . But, imagine the system evolves under a dynamics described by random variables  $\mathbf{Y}$  that are functions  $\mathbf{Y} = \mathbf{f}(\mathbf{X})$ . In this case, we can interpret the covariance matrix  $(\mathbf{C}_Y)_{kl} = \text{cov}(f_k, f_l)$  as the Fisher matrix that becomes the speed limit.

As in the pulled particle example, we recognize that quantities in the speed limit are (co)variances and use this fact to transform the speed limit. To start, we Taylor expand the  $m$  functions of  $\mathbf{f}$  in terms of  $n$  measured quantities  $\mathbf{X}$

$$f_i(\mathbf{X}) = f_i(\boldsymbol{\mu}) + \nabla f_i^\top|_{\mathbf{X}=\boldsymbol{\mu}}(\mathbf{X} - \boldsymbol{\mu}) + \mathcal{E} \quad (4)$$

with the gradient  $\nabla f_i = (\partial_{X_1} f_i, \partial_{X_2} f_i, \dots)^\top$  and error  $\mathcal{E}$ . Taking the error to be uncorrelated with the inputs  $X_i$ , the covariances between elements of  $\mathbf{X}$  propagate to the covariances of  $\mathbf{f}$

$$\mathbf{C}_Y = \nabla \mathbf{f}^\top \mathbf{C}_X \nabla \mathbf{f} + \sigma_{\mathcal{E}}^2 \quad (5)$$

under the action of the Jacobian  $\nabla \mathbf{f}$ . We can interpret this relationship as a generalization of Gauss's error propagation law [59, 66] or as the coordinate transformation

of the Fisher matrix from  $\mathbf{X}$  to  $\mathbf{Y}$  [67]. Even if the measurable variables are correlated with covariance matrix  $\mathbf{C}_X$ , one can predict the variance of several  $\mathbf{f}(\mathbf{X})$  or a single function  $Y = f(\mathbf{X})$  [68].

With Eq. (5), we can transform the scalar Fisher information that sets the speed limit. When  $Y = \hat{r}$ , the Fisher information transforms as

$$\tilde{\tau}^{-2} = \Delta \hat{r}^2 = \nabla f^\top(\mathbf{X}) \mathbf{C}_X \nabla f(\mathbf{X}). \quad (6)$$

This form of the speed limit is our main result: it transforms the directly measurable correlations between  $\mathbf{X}$  to the speed limit  $\tilde{\tau}^{-1}$ . For a single measurable quantity the Fisher information transforms from  $I_F(\theta) = (\partial_\theta f(\theta))^2 I_F(f(\theta))$  for a parameter,  $I_F(\theta)$ , to a function of that parameter,  $I_F(f(\theta)) = \Delta \theta^2$ . Equation (6) becomes Eq. (3) by recognizing that the Jacobian from  $\theta = \hat{x}$  to  $f(\theta) = \hat{r}$  is  $|\partial_{\hat{x}} \hat{r}| = |d_t \hat{x} / \Delta \hat{x}^2| = |v| / \Delta \hat{x}^2$ .

*Inferring the speed limit from data.*—All together, this transformation of the speed limit allows us to choose the input (co)variances in  $\mathbf{C}_X$  based on experimental convenience and the data that is available. As with any estimate, these choices must be made judiciously. (i) The observables, such as the heat rate  $\dot{Q} = -\text{cov}(\hat{r}, \epsilon)$ , are expressible as a covariance with the rate  $\hat{r}$  (e.g., dissipated work, chemical work, entropy production, entropy flow). The input variables are also those that are dissipative and have a finite variance; measuring fluctuations in variables that are uncorrelated with dissipative degrees of freedom would give less accurate estimates of the speed limit (SM Sec. 3).

(ii) When the distribution is Gaussian, the dragged colloidal particle is an example of the case in which  $Y = \hat{r}$  is a linear function of  $\mathbf{X} \rightarrow \hat{X}$ . However, the dynamics may not be Brownian, the distribution of  $\hat{X}$  may not be Gaussian, or the distribution may not be known analytically. Under these circumstances, the true relationship between  $\hat{r}$  and  $\hat{X}$  may be nonlinear. While a linear regression hypothesis would neglect higher order terms, a linear hypothesis will still perform well when the parameter  $b$  is constant over several  $\Delta \hat{X}$  [60]. In the nonequilibrium steady state examples here, this is a good approximation because  $b = \partial_X \hat{r}$  is a nonzero constant (i.e., the trap velocity and the time evolution of ATP concentration for the active gel below).

Even if the true relationship is nonlinear, one can still minimize the error, determine the parameters, and make an optimal prediction  $\tilde{\tau}^{-1}$  of the true speed limit  $\tau^{-1}$  with experimental data. Linear functions  $\hat{r} = a + b\hat{X}$  also have the advantage that they saturate the inequality  $\tilde{\tau}_Q^{-1} = \tilde{\tau}^{-1}$  [23] with an optimal slope  $b_{\text{opt}} = \text{cov}(\hat{X}, \hat{r}) / \Delta \hat{X}^2 = \dot{\mathcal{X}} / \Delta \hat{X}^2$  [23]. So, estimates of the speed limit are possible with linear models (avoiding the nonequilibrium probability distribution over time) when the rate  $\dot{\mathcal{X}}$  and variance  $\Delta \hat{X}^2$  are available.

(iii) Another important consideration in estimating the

speed limit from data is when the measurement overestimates the true speed limit  $\tau_O^{-1} \leq \tau^{-1} \leq \tilde{\tau}^{-1}$ . For an observable  $O$ , we found the transformed speed limit  $\tilde{\tau}^{-1}$  upper bounds the heat rate, entropy production rate, and dissipated work when the empirical standard deviation  $\Delta\hat{O}$  is larger than the true parameter  $\sigma_O$ . For example, in the pulled particle example  $O = \hat{x}$ , the ratio of the true and error propagated speed limits is

$$\frac{\tau^{-1}}{\tilde{\tau}^{-1}} = \frac{\tau^{-1}}{\tilde{\tau}^{-1}} = \frac{\sigma_x}{\Delta\hat{x}}. \quad (7)$$

This equality holds for systems with a linear or quadratic relation between  $\hat{r}$  and the experimentally accessible variable  $\hat{x}$  (SM Sec. 4-5). When  $\Delta\hat{x} > \sigma_x$ , the empirical speed limit will overestimate the true speed limit  $\tau^{-1} < \tilde{\tau}^{-1}$ , Fig. 2. The predicted speed limit is exact when there is no measurement error  $\varepsilon$  and  $\Delta\hat{x} = \sigma_x$ . For the pulled particle, the ratio of the Fisher informations satisfies this equality: The true Fisher information for the dragged particle is  $I_F = \tau^{-2} = v^2\sigma_x^2$  and the Fisher information propagated from the error in  $\hat{x}$  is  $\tilde{I}_F = \tilde{\tau}^{-1} = v^2\Delta\hat{x}^2$  (SM Sec.2). It also follows that the measurement error determines whether predictions of  $|\tilde{\dot{Q}}|$  overestimate the true heat rate  $|\dot{Q}|$ . Numerically, when the error is  $\varepsilon = +10$  nm [62], the predicted heat rate is  $|\tilde{\dot{Q}}| = 6.86 \times 10^{-20}$  W and the true value is  $|\dot{Q}| = 1.88 \times 10^{-20}$  W.

*Prediction of energy dissipation rates for active gels.*— As another example, we compared the predicted heat rate with experimental measurements for microtubule active gels. In these active materials, kinesin motors cross-link microtubule pairs. The forward motion of the motors is driven by the chemical energy from ATP hydrolysis, which also releases energy as heat and sustains self-organized flows at longer length and time scales. The first picocalorimetry measurements [12] suggest the energy efficiency of these materials is low: the minority of the input chemical energy propagating to productive emergent flows and the majority dissipated away as waste heat [11].

Using the concentrations of chemical species in our main result, Eq. (6), the predicted heat rate

$$|\tilde{\dot{Q}}| = |\partial_c \hat{r}| \Delta\hat{c} \Delta\hat{\varepsilon} = \frac{|d_t \hat{c}|}{\Delta\hat{c}} \Delta\hat{\varepsilon} \quad (8)$$

is in terms of  $|d_t \hat{c}|$  the average rate of ATP hydrolysis and the standard deviations in concentration and energy. The rate of ATP hydrolysis depends on the initial concentrations of kinesin, microtubule, ATP, and rate constants (SM Sec. 6). This rate can be determined with a previously parametrized model or without a model from the numerical derivative of concentration measurements. Here, we use measured rate constants and a kinetic model for ATP hydrolysis that were reported previously [11].

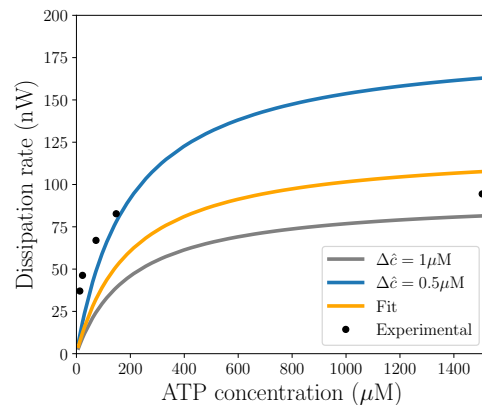


Figure 3. Comparison of predicted heat rate with experimental measurement. Averaged dissipation rate versus ATP concentration with  $[K401] = 210$  nM,  $[MT] = 16$   $\mu$ M. We use  $\Delta\hat{\varepsilon} = 10^{-8}$  W  $\times 1000$  s =  $10^{-5}$  J and the rate constants:  $k_{D,ATP} = 96.4$   $\mu$ M,  $k_{D,MT} = 17.4$   $\mu$ M, and  $k_{cat} = 44$  s $^{-1}$ . The fit (orange) is the chemical kinetics model to the data (black points) from Ref. [11].

To predict the heat rate with Eq (8), we can use either measurements or estimates of the concentration and energy fluctuations. Since there are not direct measurements of the energy fluctuations, we estimate these values from available information. The active material is in a buffer solution of 1% 35-kDa polyethylene glycol in room temperature water at a pH of 6.8 (SM Sec. 6). A single molecule undergoes about  $10^{13} - 10^{14}$  collisions per second, exchanging an average energy on the order of  $k_B T$  at a rate of  $10^{-8}$  W. In Ref. [11], the heat rate measurements are on the order of 1000 s, so we estimate  $\Delta\hat{\varepsilon} = 10^{-8}$  W  $\times 1000$  s =  $10^{-5}$  J. This estimate agrees with the uncertainty of the measured heat rate, which are on the order of 100 nW with fluctuations are on the order of 10–15 nW when the gel was prepared with and without the pyruvate kinase-based ATP regeneration system.

Pipetting error is likely the dominant source of error in these measurements [11], and data is not currently available for  $\Delta\hat{c}$ , so we instead estimate the standard deviation using experimental error. The total sample volume is 0.5  $\mu$ L and the initial ATP concentration varies from 1.5 – 1500  $\mu$ M. Propagating the 5% error in dose volume  $\Delta\hat{c} = \partial V^{-1} \Delta V$ , the uncertainty in concentration is on the order of 1  $\mu$ M for ATP concentrations in the range 12.5–190  $\mu$ M. Other potential sources of uncertainty are the pipetting protocol and fitted rate constants, which could also be accounted for using Eq. (6).

While less data is available for these estimates, they illustrate the flexibility of this method and the ability to use information on hand. With these estimated inputs, the heat rate predicted with Eq. (8) agrees well with picocalorimetry measurements [11]. Figure 3 shows the estimated heat dissipation rate as a function of ATP concentration with all other concentrations fixed. Both

the measured and estimated dissipation rates (SM Sec. 6) increase with the initial ATP concentration. Using a standard deviation for concentration  $\Delta\hat{c}$  of 0.5 or 1  $\mu\text{M}$ , the predicted heat rate is less than a factor of two of the experimental values. For low ATP concentrations, the prediction with  $\Delta\hat{c} = 0.5 \mu\text{M}$  agrees better with the measured data than the direct fit with a chemical kinetics model [11].

*Conclusions.* – Fisher information is widely used in the statistical design of experiments: with known experimental errors, one can predict *a priori* the minimum error in a measured quantity. By leveraging its appearance in the thermodynamic speed limit, we can use convenient transformations of the speed limit together with statistical regression hypotheses to predict dissipation rates. A single speed – the square root of the Fisher information – bounds multiple dissipation rates, so we expect the results here to produce estimates of other physical observables. These predictions could be useful in determining the sensitivity of measurements to experimental control variables and in determining the experimental uncertainty needed for accurate measurements of dissipation rates. Used in these ways, the thermodynamic speed limit set by the Fisher information and the transformation to more convenient variables is a potentially efficient method to guide both the design of experiments and synthetic active materials. Since these speed limit predictions of dissipation rates can be independent of an underlying microscopic model for the dynamics and the distance from thermal equilibrium, they hold across the length and time scales relevant for active materials.

## ACKNOWLEDGMENTS

We gratefully acknowledge Peter Foster and Joost Vlassak for sharing the data from Ref. [11]. This material is based upon work supported by the National Science Foundation under Grant No. 2231469.

---

\* [jason.green@umb.edu](mailto:jason.green@umb.edu)

- [1] J. Gladrow, N. Fakhri, F. C. MacKintosh, C. F. Schmidt, and C. P. Broedersz, Broken detailed balance of filament dynamics in active networks, *Physical Review Letters* **116**, 248301 (2016).
- [2] C. Battle, C. P. Broedersz, N. Fakhri, V. F. Geyer, J. Howard, C. F. Schmidt, and F. C. MacKintosh, Broken detailed balance at mesoscopic scales in active biological systems, *Science* **352**, 604 (2016).
- [3] G. Duclos, R. Adkins, D. Banerjee, M. S. Peterson, M. Varghese, I. Kolvin, A. Baskaran, R. A. Pelcovits, T. R. Powers, A. Baskaran, *et al.*, Topological structure and dynamics of three-dimensional active nematics, *Science* **367**, 1120 (2020).
- [4] E. R. Kay, D. A. Leigh, and F. Zerbetto, Synthetic molecular motors and mechanical machines, *Angewandte Chemie International Edition* **46**, 72 (2007).
- [5] S. A. P. van Rossum, M. Tena-Solsona, J. H. van Esch, R. Eelkema, and J. Boekhoven, Dissipative out-of-equilibrium assembly of man-made supramolecular materials, *Chemical Society Reviews* **46**, 5519 (2017).
- [6] G. Ragazzon and L. J. Prins, Energy consumption in chemical fuel-driven self-assembly, *Nature Nanotechnology* **13**, 882 (2018).
- [7] K. Das, L. Gabrielli, and L. J. Prins, Chemically fueled self-assembly in biology and chemistry, *Angewandte Chemie International Edition* **60**, 20120 (2021).
- [8] E. Del Grosso, E. Franco, L. J. Prins, and F. Ricci, Dissipative DNA nanotechnology, *Nature Chemistry* **14**, 600 (2022).
- [9] D. Barpuzary, P. J. Hurst, J. P. Patterson, and Z. Guan, Waste-free fully electrically fueled dissipative self-assembly system, *Journal of the American Chemical Society* **145**, 3727 (2023).
- [10] O. E. Shklyaeu and A. C. Balazs, Interlinking spatial dimensions and kinetic processes in dissipative materials to create synthetic systems with lifelike functionality, *Nature Nanotechnology* **19**, 146 (2024).
- [11] P. J. Foster, J. Bae, B. Lemma, J. Zheng, W. Ireland, P. Chandrakar, R. Boros, Z. Dogic, D. J. Needleman, and J. J. Vlassak, Dissipation and energy propagation across scales in an active cytoskeletal material, *Proceedings of the National Academy of Sciences* **120**, e2207662120 (2023).
- [12] J. Bae, J. Zheng, H. Zhang, P. J. Foster, D. J. Needleman, and J. J. Vlassak, A micromachined picocalorimeter sensor for liquid samples with application to chemical reactions and biochemistry, *Advanced Science* **8**, 2003415 (2021).
- [13] A. Rizvi, J. T. Mulvey, B. P. Carpenter, R. Talosig, and J. P. Patterson, A close look at molecular self-assembly with the transmission electron microscope, *Chemical Reviews* **121**, 14232 (2021).
- [14] Z. G. Nicolaou and A. E. Motter, Missing links as a source of seemingly variable constants in complex reaction networks, *Phys. Rev. Res.* **2**, 043135 (2020).
- [15] T. van Leeuwen, A. S. Lubbe, P. Štacko, S. J. Wezenberg, and B. L. Feringa, Dynamic control of function by light-driven molecular motors, *Nature Reviews Chemistry* **1**, 0096 (2017).
- [16] E. Moulin, L. Faour, C. C. Carmona-Vargas, and N. Giuseppone, From molecular machines to stimuli-responsive materials, *Advanced Materials* **32**, 1906036 (2020).
- [17] L. Zhang, Y. Qiu, W.-G. Liu, H. Chen, D. Shen, B. Song, K. Cai, H. Wu, Y. Jiao, Y. Feng, *et al.*, An electric molecular motor, *Nature* **613**, 280 (2023).
- [18] L. Peliti and S. Pigolotti, *Stochastic Thermodynamics* (Princeton University Press, 2021).
- [19] S. B. Nicholson, L. P. García-Pintos, A. del Campo, and J. R. Green, Time-information uncertainty relations in thermodynamics, *Nature Physics* **16**, 1211 (2020).
- [20] R. A. Fisher, Theory of statistical estimation, in *Mathematical proceedings of the Cambridge philosophical society*, Vol. 22 (Cambridge University Press, 1925) pp. 700–725.
- [21] E.-j. Kim, Information geometry, fluctuations, non-equilibrium thermodynamics, and geodesics in complex systems, *Entropy* **23**, 1393 (2021).

- [22] B. R. Frieden, *Science from Fisher information*, Vol. 974 (Citeseer, 2004).
- [23] S. B. Nicholson and J. R. Green, [Thermodynamic speed limits from the regression of information](#) (2021), [arXiv:2105.01588 \[cond-mat.stat-mech\]](#).
- [24] E. Aghion and J. R. Green, Relations between timescales of stochastic thermodynamic observables, *Journal of Non-Equilibrium Thermodynamics* **48**, 10.1515/jnet-2022-0104 (2023).
- [25] E. Aghion and J. R. Green, Thermodynamic speed limits for mechanical work, *Journal of Physics A: Mathematical and Theoretical* **56**, 05LT01 (2023).
- [26] Y. Oono and M. Paniconi, Steady state thermodynamics, *Progress of Theoretical Physics Supplement* **130**, 29 (1998).
- [27] If no work is done on or by the system, then a simpler result holds [69].
- [28] S. Deffner and E. Lutz, Quantum speed limit for non-Markovian dynamics, *Physical Review Letters* **111**, 010402 (2013).
- [29] T. Fogarty, S. Deffner, T. Busch, and S. Campbell, Orthogonality catastrophe as a consequence of the quantum speed limit, *Physical Review Letters* **124**, 110601 (2020).
- [30] S. Deffner, Quantum speed limits and the maximal rate of information production, *Physical Review Research* **2**, 013161 (2020).
- [31] S. Das and J. R. Green, Speed limits on deterministic chaos and dissipation, *Physical Review Research* **5**, L012016 (2023).
- [32] S. Das and J. R. Green, Maximum speed of dissipation, *Physical Review E* **109**, L052104 (2024).
- [33] N. Shiraishi, K. Funo, and K. Saito, Speed limit for classical stochastic processes, *Physical Review Letters* **121**, 070601 (2018).
- [34] S. B. Nicholson, A. del Campo, and J. R. Green, Nonequilibrium uncertainty principle from information geometry, *Physical Review E* **98**, 032106 (2018).
- [35] Y. Hasegawa and T. Van Vu, Uncertainty relations in stochastic processes: An information inequality approach, *Physical Review E* **99**, 062126 (2019).
- [36] G. Falasco and M. Esposito, Dissipation-time uncertainty relation, *Physical Review Letters* **125**, 120604 (2020).
- [37] A. C. Barato and U. Seifert, Thermodynamic uncertainty relation for biomolecular processes, *Physical Review Letters* **114**, 158101 (2015).
- [38] T. R. Gingrich and J. M. Horowitz, Fundamental bounds on first passage time fluctuations for currents, *Physical Review Letters* **119**, 170601 (2017).
- [39] J. Li, J. M. Horowitz, T. R. Gingrich, and N. Fakhri, Quantifying dissipation using fluctuating currents, *Nature Communications* **10**, 1666 (2019).
- [40] J. M. Horowitz and T. R. Gingrich, Thermodynamic uncertainty relations constrain non-equilibrium fluctuations, *Nature Physics* **16**, 15 (2020).
- [41] S. K. Manikandan, D. Gupta, and S. Krishnamurthy, Inferring entropy production from short experiments, *Physical review letters* **124**, 120603 (2020).
- [42] S. Otsubo, S. Ito, A. Dechant, and T. Sagawa, Estimating entropy production by machine learning of short-time fluctuating currents, *Physical Review E* **101**, 062106 (2020).
- [43] T. Van Vu, V. T. Vo, and Y. Hasegawa, Entropy production estimation with optimal current, *Physical Review E* **101**, 042138 (2020).
- [44] A. Pal, S. Reuveni, and S. Rahav, Thermodynamic uncertainty relation for first-passage times on Markov chains, *Physical Review Research* **3**, L032034 (2021).
- [45] A. Dechant and S.-i. Sasa, Improving thermodynamic bounds using correlations, *Physical Review X* **11**, 041061 (2021).
- [46] P. Pietzonka and F. Coghi, [Thermodynamic cost for precision of general counting observables](#) (2023), [arXiv:2305.15392 \[cond-mat.stat-mech\]](#).
- [47] J. Lyu, K. J. Ray, and J. P. Crutchfield, [Entropy production by underdamped Langevin dynamics](#) (2024), [arXiv:2405.12305 \[cond-mat.stat-mech\]](#).
- [48] D. J. Skinner and J. Dunkel, Estimating entropy production from waiting time distributions, *Physical Review Letters* **127**, 198101 (2021).
- [49] E. Nitzan, A. Ghosal, and G. Bisker, Universal bounds on entropy production inferred from observed statistics, *Physical Review Research* **5**, 043251 (2023).
- [50] J. van der Meer, B. Ertel, and U. Seifert, Thermodynamic inference in partially accessible Markov networks: A unifying perspective from transition-based waiting time distributions, *Physical Review X* **12**, 031025 (2022).
- [51] I. Di Terlizzi, M. Gironella, D. Herráez-Aguilar, T. Betz, F. Monroy, M. Baiesi, and F. Ritort, Variance sum rule for entropy production, *Science* **383**, 971 (2024).
- [52] I. D. Terlizzi, M. Baiesi, and F. Ritort, Variance sum rule: proofs and solvable models, *New Journal of Physics* **26**, 063013 (2024).
- [53] P. E. Harunari, A. Dutta, M. Poletti, and E. Roldán, What to learn from a few visible transitions' statistics?, *Physical Review X* **12**, 041026 (2022).
- [54] K. Blom, K. Song, E. Vouga, A. Godec, and D. E. Makarov, Milestoning estimators of dissipation in systems observed at a coarse resolution, *Proceedings of the National Academy of Sciences* **121**, e2318333121 (2024).
- [55] L. Mandelstam and I. G. Tamm, The uncertainty relation between energy and time in non-relativistic quantum mechanics, in *Selected Papers*, edited by I. E. Tamm, B. M. Bolotovskii, V. Y. Frenkel, and R. Peierls (Springer, Berlin, Heidelberg, 1991) pp. 115–123.
- [56] L. P. Garcia-Pintos, S. B. Nicholson, J. R. Green, A. del Campo, and A. V. Gorshkov, Unifying quantum and classical speed limits on observables, *Physical Review X* **12**, 011038 (2022).
- [57] Y. Jung and I. Lee, Optimal design of experiments for optimization-based model calibration using Fisher information matrix, *Reliability Engineering & System Safety* **216**, 107968 (2021).
- [58] D. Berengut, *Statistics for experimenters: Design, innovation, and discovery* (2006).
- [59] C.-F. Gauss, *Theoria combinationis observationum erroribus minimis obnoxiae* (Henricus Dieterich, 1823).
- [60] R. J. Barlow, *Statistics: a guide to the use of statistical methods in the physical sciences*, Vol. 29 (John Wiley & Sons, 1993).
- [61] A. Imparato, L. Peliti, G. Pesce, G. Rusciano, and A. Sasso, Work and heat probability distribution of an optically driven Brownian particle: Theory and experiments, *Physical Review E* **76**, 050101 (2007).
- [62] F. Ritort, Single-molecule experiments in biological physics: methods and applications, *Journal of Physics: Condensed Matter* **18**, R531 (2006).
- [63] With these numerical values of radius and viscosity, the inverse friction coefficient is  $\gamma = 5.30 \times 10^7 \text{ m N}^{-1} \text{ s}^{-1}$ .

- [64] T. Speck, J. Mehl, and U. Seifert, Role of external flow and frame invariance in stochastic thermodynamics, *Physical Review Letters* **100**, 178302 (2008).
- [65] In the comoving frame [70], the position is initially delta function distributed  $\rho(x-vt_0) = \delta(x-x(t_0))$  and eventually evolves as  $\rho(x-vt) = e^{-|x-vt|^2/2\sigma_x^2}/\sqrt{2\pi\sigma_x^2}$  at steady state.
- [66] P. Bevington and D. K. Robinson, *Data Reduction and Error Analysis for the Physical Sciences*, 3rd ed. (McGraw-Hill Education, Boston, Mass., 2002).
- [67] E. L. Lehmann and G. Casella, *Theory of Point Estimation*, 2nd ed. (Springer, New York, 1998).
- [68] Standard propagation of error is a simple approximation of the distribution  $\rho_Y(y)$  of  $Y$  with only the first two moments,  $\mu_Y$  and  $\sigma_Y^2$ : Gauss's error propagation law [59] predicts the variance  $\sigma_Y^2 = \sigma_X^2 (\partial_X f|_{X=\mu_X})^2$  and the Taylor expansion  $Y = f(\mu_X) + \partial_X f|_{X=\mu_X} (X - \mu_X)$  predicts the mean  $\mu_Y = f(\mu_X)$ . It is a special case in which the function  $f$  is linear, making the error  $\varepsilon = 0$  and  $\sigma_\varepsilon^2 = 0$ .
- [69] S. Ito and A. Dechant, Stochastic time evolution, information geometry, and the Cramér-Rao bound, *Physical Review X* **10**, 021056 (2020).
- [70] R. van Zon and E. G. D. Cohen, Extended heat-fluctuation theorems for a system with deterministic and stochastic forces, *Physical Review E* **69**, 056121 (2004).